

Institutions and the transmission of upper-tail human capital: scientific lineages across a millennium

Hiroyuki Chuma^{*1}, Kanji Otsuka², and Yoichi Sato³

¹Institute of Innovation Research, Hitotsubashi University

²Professor Emeritus, Meisei University

³Shuhari System

June 1, 2026

Abstract

What made useful knowledge cumulative was not discovery alone but the institutions that transmitted it. We provide the first exhaustive structural measurement of the network through which upper-tail human capital passed from master to student across a millennium. Using 470,000 mentor–student records from Wikidata (which integrates the Mathematics Genealogy Project and MacTutor Archive), and all 64 historical Fields Medalists as a fixed, *ex ante* tracer set, backward traversal yields a directed acyclic graph of 25.5 million paths reaching 57 generations. We document two institutional transitions. First, a 17th-century watershed concentrates lineage traffic on Leibniz: 47 of 64 lineages pass through him with a 10:1 downstream-to-upstream ratio, and seven independent attributes—learned-society membership (a 46-fold rise per scholar), field, language, employer, institutional diversification, student production, and diffusion entropy—re-organize coherently across the same window. This is the network signature of Mokyr’s Republic of Letters, and it reframes the Newton–Leibniz priority dispute as a distinction between the *possession* and the *transmission* of upper-tail human capital: it is transmission that generates the spillovers on which growth depends. Second, 84% of lineages converge upstream on five 12th–13th-century Islamic and Byzantine scholars before terminating at an 11th-century boundary—the “Monastery Wall”—at which personal academic mentorship first becomes record-generating in Europe. Our claims are descriptive-structural, not causal. Because exhaustive traversal at this scale defeats standard tools, we also contribute a deterministic, algebraic graph-traversal instrument whose measurement bias we characterize in closed form, and report one emergent property of independent methodological interest.

JEL classification: N01; O33; O43; J24; C81; Z13.

Keywords: Knowledge transmission; Human capital; Institutions; Scientific networks; Cliometrics; Computational history.

*Corresponding author: chuma@iir.hit-u.ac.jp. Institute of Innovation Research, Hitotsubashi University, 2-1 Naka, Kunitachi, Tokyo 186-8603, Japan.

1 Introduction

What enabled the sustained accumulation of the “useful knowledge” on which modern economic growth depends? Mokyr (2002, 2016) argues that the answer lies not in any single discovery but in the institutions—universities, learned societies, journals, correspondence networks—that made knowledge transmittable across generations and borders, with the 17th–18th-century Republic of Letters as the critical innovation. A complementary literature locates the engine of growth specifically in the upper tail of the human-capital distribution: Squicciarini and Voigtländer (2015) show that it is the density of knowledge elites, not average literacy, that predicts industrial growth in the age of Enlightenment. Yet the object common to both arguments—the network through which upper-tail human capital actually moved from master to student, across civilizations and across the porous boundaries between mathematics, natural philosophy, and astronomy that characterized the pre-modern learned world—has remained essentially unmeasured at scale.

This paper measures it. Our contribution is, first, a body of new structural facts about that network, and second, a measurement strategy that makes such facts obtainable. Existing empirical work on the economic history of knowledge has measured narrow windows with specific proxies: Squicciarini and Voigtländer (2015) on *Encyclopédie* subscriptions, Dittmar (2011) on the printing press, Cantoni and Yuchtman (2014) on medieval universities. These designs achieve causal identification within a bounded setting. The aggregate transmission network—how many routes connected past to present across a full millennium, where they converged, where they broke—calls for a different and complementary mode: exhaustive rather than sampled, structural rather than episodic, spanning a millennium rather than a decade. We are explicit at the outset that the resulting facts are descriptive-structural, not causal estimates. We regard this as the appropriate scope for a first map of an object this large, and as a precondition for—not a substitute for—identified work that would treat transmission costs as endogenous.

We document two transitions in the social architecture of transmission. The first, at the 17th-century Leibnizian watershed, is a re-organization of knowledge production within an already-existing institutional regime. The second, at the 11th century, is a more foundational shift in the medium of transmission—from communal monastic education to personal academic lineage—which we name the *Monastery Wall* after the network-legible signature it leaves. Each is a structural property of a 25.5-million-path network we reconstruct for the first time.

We use the complete set of historical Fields Medalists (64 laureates) solely as a tracer set: a uniform, *ex ante* criterion for which present-day research lineages to follow backward through the mentor–student relation. The Medal is not a claim about the primacy of mathematics; in Wikidata, which integrates the Mathematics Genealogy Project (P549) and the MacTutor Archive (P1563), the field label is a coarse modern tag that loses disciplinary purity upstream. The point of a fixed starting set is replicability: any reader can recover which nodes seed the 25.5 million paths, while the findings concern the shape of the entire induced subgraph. A different tracer set (say, Nobel laureates in physics) would change absolute counts but not the question the exercise makes well posed: where, on a graph too large for unaided historical intuition, does the topology concentrate?

A measurement obstacle had to be cleared first. Academic genealogy on Wikidata’s 470,000-record graph is a directed acyclic graph whose distinct paths grow multiplicatively with depth, reaching 25.5 million at generation 57; the standard lookup primitives of computational social

science exhaust memory far below this frontier size¹, and standard graph centralities are semantically blind to field. We therefore built a deterministic, algebraic graph-traversal instrument (VaCoAl/PyVaCoAl). Because building the instrument was integral to the measurement, we present it in the body (Section 2.4) rather than as a black box: we report its architecture, its biases, and one emergent property—an instrument-level path-dependence that, on reflection, sharpens rather than confounds the historical reading—and give the full algorithmic specification in the Appendix. A reader interested only in the historical findings may take from Section 2.4 the single fact that the instrument’s measurement error is bounded in closed form and is overwhelmed by the first-order results.

2 The structure of a millennium of transmission

2.1 The 17th-century watershed: an hourglass at Leibniz

Genealogical traffic centered on Leibniz forms a canonical hourglass (Fig. 1): a thin band of mid-stream positions concentrates traffic while wide sets of more distant nodes feed in from the past and diffuse out toward the present. A scholar who both draws from a diverse upstream pool and scatters that inheritance across a diverse downstream pool acts as a re-publication device for the entire graph; the hourglass is the macroscopic signature of a teacher whose intellectual descendants remain visible for centuries.

Upstream nodes carry an average of 5.3 traversing paths; downstream, the figure expands to 53.4—a thickness ratio of $10.1\times$ (Table 1). Newton’s profile is the stark contrast: only four Fields Medalists trace their genealogy through Newton, and his node shows no constriction-and-explosion pattern in either direction. This is not a valuation of “German networking” over “English genius”; it is a property of a directed graph built from a single predicate, and the appropriate comparison is between two figures who both carry enormous semantic weight in the history of the calculus yet differ sharply in the depth and width of the lineages documented through them.

What Leibniz built was an apparatus of transmission: he founded the Berlin Academy of Sciences in 1700, maintained one of the largest scholarly correspondence networks in Europe, and initiated an academic lineage running through Johann Bernoulli, Euler, Lagrange, Laplace, and Poisson. Newton, for all his genius, operated largely in isolation and trained few successors. Other hubs (Euler, Gauss, Hilbert; Table 1) also exhibit high thickness ratios, but Leibniz combines a large absolute path count with the 10 : 1 asymmetry, reflecting the scale of the lineage that actually passes through him.

The 300-year priority dispute over the calculus (Hall, 1980) turned on a question—who discovered first?—to which our instrument can add no evidence. It can, however, reframe the question in economic terms. Rather than asking who possessed the intellectual content first, we ask who built the transmission infrastructure. We construct a composite *Giant Score*

$$G(v) = \hat{s}(v) \cdot \hat{t}(v), \quad \hat{s}(v) = \max(s(v) - 0.5, 0) \times 10, \quad (1)$$

where $\hat{s}(v)$ is a measure of the node’s calculus-semantic content and $\hat{t}(v)$ is its path count to the 64 Fields Medalists, normalized by the maximum (construction in Appendix D). Only scholars

¹In our PyVaCoAl application, the Frontier Size (FS) bounds the number of concurrent paths tracked during retrieval, preventing combinatorial explosion during branching reasoning.

high on *both* dimensions rank at the top (Table 2). Newton ranks 91st despite a calculus-content score of 0.534, almost indistinguishable from Leibniz’s 0.569; his low rank is driven entirely by a path count of four. Read through the upper-tail human-capital framework of Squicciarini and Voigtländer (2015), the table operationalizes a distinction long latent in the history of science: between the *possession* and the *transmission* of upper-tail human capital. Newton possessed the calculus; Leibniz possessed *and* transmitted it. It is transmission, not possession, that generates the human-capital spillovers on which sustained growth depends, and reframed this way the dispute admits a quantitative answer the priority frame by construction cannot offer.

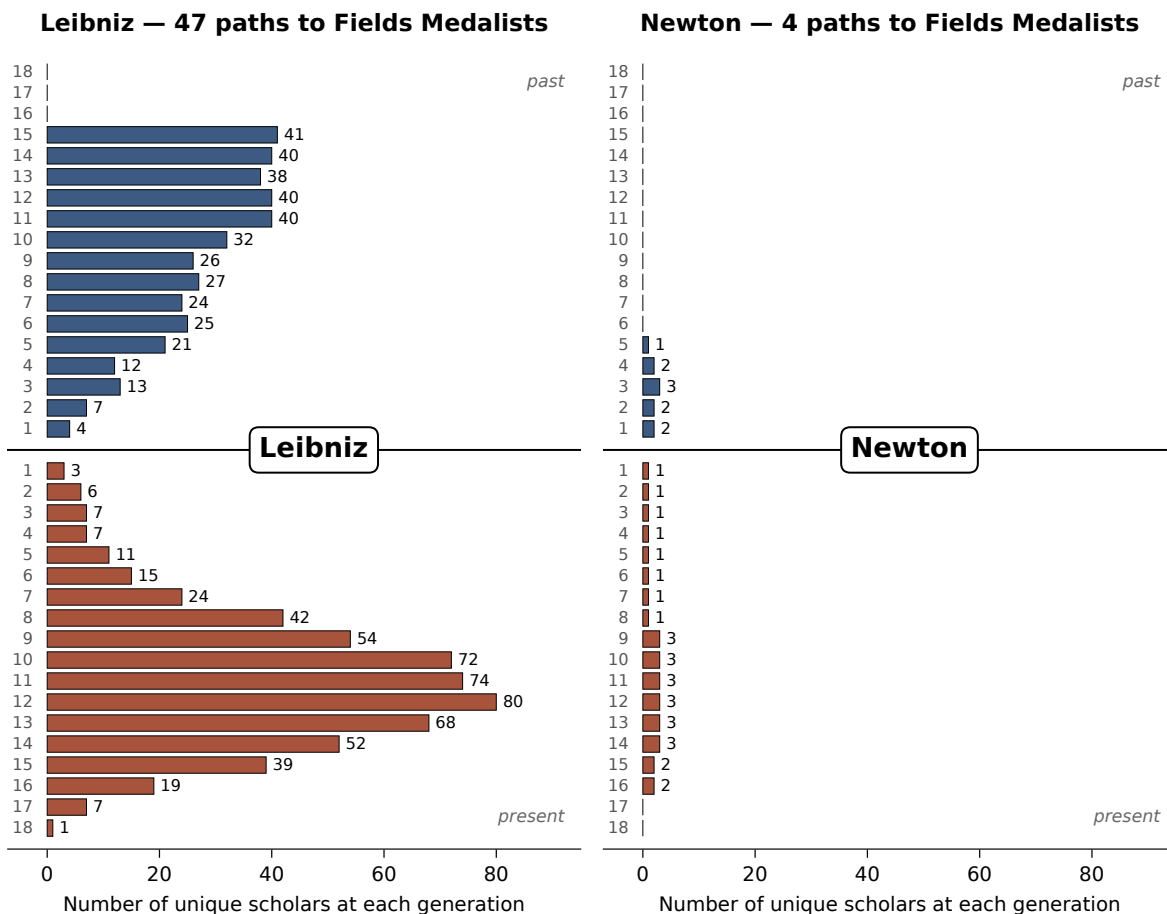


Figure 1: **Hourglass topology of genealogical traffic.** Leibniz (top) versus Newton (bottom), drawn to the same scale. Each bar is the number of unique scholars at a given generational distance through which paths to Fields Medalists pass. Upper half: mentor direction (past); lower half: student direction (present). The number to the left of each bar is the generational distance; to the right, the hub count. Leibniz exhibits the canonical hourglass; Newton’s profile is a thin thread with no hub structure in either direction.

2.2 The Republic of Letters as a multi-predicate institutional transition

If the 17th-century watershed reflects the formation of a more durable transmission infrastructure, the change should appear not only in path counts but across independent attributes of scholarly activity. We compare pre- and post-Leibniz windows within the induced subgraph using seven indicators drawn from orthogonal predicate dimensions (Table 3). The question

Table 1: Path counts and thickness ratios at hub nodes.

| Hub | Mentor avg. paths | Student avg. paths | Ratio |
|---------|-------------------|--------------------|-------|
| Leibniz | 5.3 | 53.4 | 10.1× |
| Gauss | 2.7 | 41.2 | 15.1× |
| Hilbert | 1.6 | 29.2 | 18.5× |
| Euler | 3.6 | 52.4 | 14.6× |
| Newton | ~1 | ~2 | — |

Table 2: Giant Score: combining semantic content with structural position.

| Rank | Scholar (dates) | Score | Calc. Degree | Paths |
|------|--------------------------|-------|--------------|-------|
| 1 | J. F. Pfaff (1765–1825) | 0.841 | 0.638 | 33 |
| 2 | Leibniz (1646–1716) | 0.597 | 0.569 | 47 |
| 3 | J. Bernoulli (1655–1705) | 0.423 | 0.551 | 45 |
| 12 | Euler (1707–1783) | 0.244 | 0.529 | 45 |
| 17 | Gauss (1777–1855) | 0.167 | 0.531 | 29 |
| 91 | Newton (1643–1727) | 0.025 | 0.534 | 4 |

is whether a coherent cluster of fields, languages, employers, and voluntary associations reorganizes around Leibniz without erasing the earlier layers of the network.

The strongest single indicator is learned-society membership. Before the Leibniz window, 6.5% of scholars in the network held recorded society memberships, averaging 0.08 per person; after Leibniz, the rate rose to 82.1%, averaging 3.81 per person—a 46× increase. This is the most direct network analogue of Mokyr’s argument: voluntary scholarly associations became part of the durable infrastructure through which knowledge circulated. The three continuity indicators (field, language, employer) each measure how much the composition of academic activity changed from the pre- to the post-period; all three exceed the no-change baseline of 0.5 (0.614, 0.603, 0.603), indicating *continuous transformation*—the cluster centered on calculus developed and differentiated through Leibniz rather than replacing what came before. That three independent dimensions exhibit this pattern simultaneously shows the shift pervaded the whole social infrastructure of knowledge production: not merely what was studied, but how, where, and in what language it was communicated. The Student Top-Tier Production Rate of 1.000—every one of Leibniz’s direct students generated descendants reaching the highest tier of network influence—is the signature of a self-sustaining transmission infrastructure. The joint movement of seven indicators across orthogonal dimensions establishes a system-level institutional transition, not an artefact of better modern documentation in any single dimension.

2.3 Upstream convergence and the Monastery Wall

We now turn upstream of the Leibniz watershed. Among the 213 individuals with the maximum path count of 54 (surpassing even Leibniz), five Islamic scholars of the 12th–13th centuries emerge as the furthest-upstream hubs of the entire network (Table 4). The chain terminates with Grigorios Choniades, a Byzantine scholar who studied in Persia and carried Islamic astronomical and mathematical knowledge back to the Greek-speaking world.

Table 3: Indicators of institutional transformation centered on Leibniz.

| Indicator | Value | Evidence |
|------------------------------|--|-------------|
| Society explosion (Post/Pre) | 0.08 \rightarrow 3.81 (46 \times) | Strong |
| Field continuity | 0.614 | Strong |
| Language continuity | 0.603 | Strong |
| Employer continuity | 0.603 | Strong |
| Inst. hub diversification | 2.5 \times | Moderate |
| Student top-tier rate | 100% | Very strong |
| Influence diffusion entropy | 3.401 | Very strong |

That 54 of 64 Fields Medalists (84.4% at our reference frontier size $FS = 20,000$) trace genealogies converging on five individuals constituting less than 0.001% of the database reveals a striking path-dependency in documented human-capital transmission. Stated at this magnitude the finding is not a counterfactual claim that “Islamic science caused Fields Medals”; it is the claim that, on the only relation we observe at scale, a microscopic slice of the node set carries an overwhelming share of the paths on which the tracer set depends. This is consistent with the qualitative arguments of Saliba (2007) and Itoh (1993), to which it adds a quantitative structural dimension. The figure is a lower bound in two senses: it is frontier-size-dependent, and Wikidata is biased toward the Western archive and the doctoral-advisor idiom, so genuine debts to figures absent from the graph can only dilute the apparent share of any chokepoint in future, richer data.

The mentor–student predicate captures only one channel of transmission. The 12th-century Great Translation Movement—in which Arabic renderings of Greek originals and original Arabic works were translated into Latin at Toledo, Sicily, and northern Italy (Itoh, 1993)—moved knowledge through books and translators, not personal mentorship, and is by construction invisible to a mentor–student genealogy. A further contribution of this paper is to show that it is not invisible to *semantic* analysis of the network’s nodes. Using the instrument’s Unbinding operation to extract the field component from each node’s composite vector and tracking 50-year windows from 1100 to 1800, we detect a coherent Toledo–Maragha astronomy signal during 1250–1300 (+0.0025 relative to base) and a stronger Renaissance signal during 1450–1500 (+0.0065, coinciding with Copernicus’s lifetime), while algebra remains within ± 0.001 of the random baseline of 0.5 across the same windows (Table 5). The window construction, the Unbinding operation, and the corroboration with Holy-Roman-Empire language-shift data are detailed in Appendix H.

Why does the chain terminate with the five Islamic scholars rather than continuing? Despite exhaustive parameter exploration, no genealogy extends beyond the 57th generation. Every path terminates at one of two figures who predate the five by roughly a century: Archbishop Lanfranc of Canterbury (1005–1089), who taught at the Abbey of Bec, or Ivo of Chartres (1040–1116); their own mentors are unrecorded. We term this systematic cessation the *Monastery Wall*. As Rashdall (2010) and De Ridder-Symoens (1992) document, education in the 10th and 11th centuries revolved around *scholae monasticae* and cathedral schools, where the monastic ideal of *stabilitas loci* made education a communal affair oriented toward scriptural understanding—channels that by their nature generated no structured mentor–student records. The 11th-century

shift from this regime to the personal academic lineages of the cathedral schools and nascent universities is the supply-side complement to the demand-side transition that Cantoni and Yuchtman (2014) study.

The chronological profile of the 213 maximum-path scholars makes the boundary visible at the population level: a single 11th-century entry (Lanfranc), only 13 individuals in the 12th century, a ramp through the scholastic 13th–15th centuries, a peak at the 16th-century inception of the Scientific Revolution (37.1% of the 213), and a 17th-century tail after which Leibniz alone carries the maximum. The single 11th-century entry is not a statistical anomaly but the literal Monastery-Wall boundary in the data: the earliest scholar at whom the personal-mentorship chain still attaches to a name on record. Where the 17th-century watershed was a shift in the social architecture of production within an existing regime, the 11th-century transition was a shift in the medium of transmission itself. The Islamic convergence and the Monastery Wall are, in this sense, two faces of one institutional discontinuity: modern lineages pass through these five scholars because, on the far side of them, “personal mentorship” had not yet crystallized into a record-generating institution in Europe; on the near side, it had.

Table 4: The five Islamic and Byzantine scholars at the headwaters of the Fields Medalist genealogy, in order of mentor-to-student succession. All five lie on the chain through which 54 of 64 Fields Medalists trace their genealogy.

| Order | Scholar | Dates; Birthplace | Paths |
|-------|-------------------------|---------------------------|-------|
| 1 | Sharaf al-Dīn al-Ṭūsī | 1135–1201; Tus (Iran) | 54 |
| 2 | Kamāl al-Dīn bin Yūnis | 1156–1242; Mosul | 54 |
| 3 | Naṣīr al-Dīn al-Ṭūsī | 1201–1274; Tus (Iran) | 54 |
| 4 | Shams al-Dīn al-Bukhārī | 1254–1300; Bukhara | 54 |
| 5 | Grigorios Choniades | 1240–1320; Constantinople | 54 |

2.4 The instrument as a finding, and a robustness analysis

The findings so far are about the historical network. An unanticipated finding concerns the instrument, and proves on reflection to be also about the history. The VaCoAl architecture includes a block-level collision-tolerance mechanism (“Don’t Care”) that suppresses block votes when two distinct items map to the same address. In single-step retrieval this guards against false majorities; under iterative multi-hop traversal it acquires a second-order effect we did not anticipate.

Per-step confidence CR_1 at sufficient memory depth stabilizes slightly below unity—in our experiments $CR_1 \approx 0.997$. Because the path-integral score accumulates as

$$CR_2(n) = CR_2(n-1) \cdot CR_1(n-1), \quad (2)$$

the deviation compounds exponentially with generational distance, $CR_2(n) \approx CR_1^n$, so that at $n = 56$, $CR_2 \approx 0.997^{56} \approx 0.846$. On 25.5 million real paths through a 57-generation DAG we measure $CR_2 \approx 0.905$ at generation 56—of the same order as the closed-form prediction, with the residual gap consistent with survivor bias along deep paths (Fig. 2).

The within-frontier ranking of candidates is therefore not arbitrary: short, direct genealogical routes accumulate less penalty than circuitous, long ones, and the instrument selects them

Table 5: Rate of HDC signal change between adjacent 50-year windows for algebra and astronomy, extracted via Unbinding of the field component from the composite hyperdimensional vector of all scholars active in each window. \blacktriangle / ∇ mark notable increases / decreases. Astronomy departs upward in two windows aligned with the second Toledo translation period (1250–1300) and the Copernican Renaissance (1450–1500); algebra remains near the baseline of 0.5.

| Window | Algebra | | Astronomy | |
|-----------|---------|--------------------------|-----------|--|
| | Signal | Δ | Signal | Δ |
| 1100–1150 | 0.4999 | (base) | 0.5003 | (base) |
| 1150–1200 | 0.5001 | +0.0001 | 0.4999 | −0.0003 |
| 1200–1250 | 0.4998 | −0.0003 | 0.4999 | ~ 0 |
| 1250–1300 | 0.4997 | −0.0001 | 0.5024 | +0.0025 $\blacktriangle\blacktriangle$ |
| 1300–1350 | 0.5001 | +0.0004 | 0.5021 | −0.0003 |
| 1350–1400 | 0.5000 | −0.0001 | 0.4994 | −0.0027 $\nabla\nabla$ |
| 1400–1450 | 0.4995 | −0.0004 | 0.4987 | −0.0007 |
| 1450–1500 | 0.4994 | −0.0001 | 0.5052 | +0.0065 $\blacktriangle\blacktriangle\blacktriangle\blacktriangle\blacktriangle\blacktriangle$ |
| 1500–1550 | 0.5003 | +0.0009 | 0.5033 | −0.0019 ∇ |
| 1550–1600 | 0.4996 | −0.0007 | 0.5039 | +0.0006 |
| 1600–1650 | 0.5001 | +0.0005 | 0.5076 | +0.0037 $\blacktriangle\blacktriangle\blacktriangle$ |
| 1650–1700 | 0.5019 | +0.0018 \blacktriangle | 0.5053 | −0.0023 $\nabla\nabla$ |
| 1700–1750 | 0.5006 | −0.0013 ∇ | 0.5050 | −0.0002 |
| 1750–1800 | 0.5010 | +0.0004 | 0.5079 | +0.0029 $\blacktriangle\blacktriangle$ |

accordingly—a *structural Occam’s razor*. This emergent property is functionally analogous to spike-timing-dependent plasticity in biological neural circuits (Bi and Poo, 1998): connections reinforced by short, direct sequences strengthen while those traversed only through long, circuitous chains weaken. We did not design this in; the algebraic collision-tolerance mechanism, combined with the multiplicative structure of CR_2 , generates it. The behavior is not a single-configuration coincidence: sweeping the block count N from 64 to 1024 under the fixed total-capacity constraint $N \cdot 2^m = 2^{34}$, CR_1 remains above 0.975 throughout while CR_2 traces a family of decay curves encoding the trade-off between orthogonal resolution (scaling with N) and per-block collision tolerance (scaling with 2^m); the single configuration that matches the maximum genealogical depth of 57 generations is $N = 512$ (Fig. 3), a phase-transition signature rather than a tuning artefact, and the strongest internal evidence that the historical findings are not balanced on a particular parameter choice.

This finding is consequential for historical interpretation, and it is also the part of the paper most likely to invite skepticism. A reasonable concern is whether the extreme path-dependence we report—84% of genealogies through five individuals, the 10 : 1 hourglass asymmetry—is a property of history or an artefact of an instrument that itself generates path-dependence. Four points respond, in decreasing order of abstraction.

Scale: the instrument’s path-dependence operates at $O(10^{-3})$ per-step deviations; the historical path-dependence operates at 54/64 Medalists and ratios of 10:1 and 46:1—not quantities the instrument could conjure. *Shape*: the instrument’s decay is smooth and monotonic along generational distance; the historical findings exhibit discrete structural discontinuities (a wall

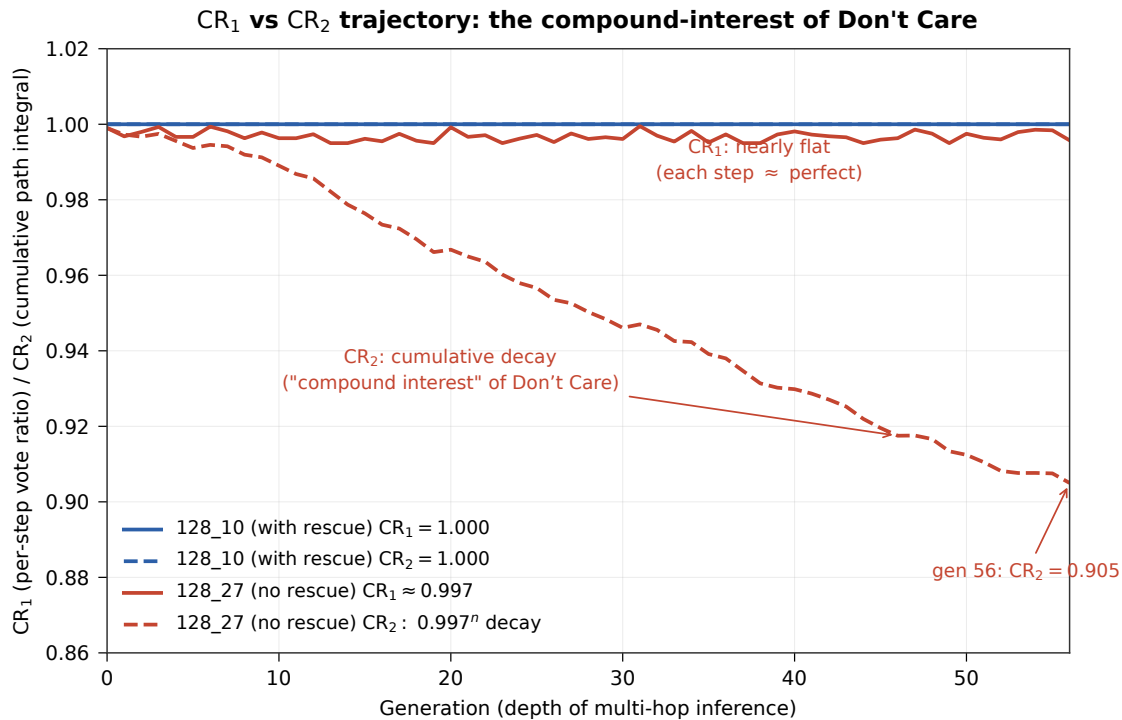


Figure 2: **Generational trajectories of CR_1 and CR_2 .** PyVaCoAl in the 128_27 configuration (without rescue; main analysis) versus 128_10 (with rescue). In 128_27 the per-generation CR_1 stays within 0.995–0.999, so single-step retrieval is near-perfect, but CR_2 decays monotonically, reaching ≈ 0.905 at the 56th generation. In 128_10 with rescue, both are pinned at 1.0, suppressing the emergent selection mechanism entirely.

at the 11th century, a bottleneck at five 12th-century individuals, a watershed at 1700) with no analogue in the instrument’s internal dynamics. *Switchability*: the Rescue-mode configuration (which pins $CR_1 = 1.0$ and eliminates the emergent penalty entirely) produces the same Leibniz hourglass, the same Republic-of-Letters indicators, the same Islamic convergence, the same Monastery Wall; the historical findings are visible with or without the mechanism. *Direction*: the emergent mechanism acts as an Occam’s razor on the candidate ordering *within* each frontier, not on the selection of the frontier itself.

That the macro-structures survive switching off the razor (Rescue mode) demonstrates that it refines rather than generates them. In Don’t Care mode it sharpens the within-frontier ranking so that short, direct, semantically coherent lineages rise above deep, circuitous ones: under PyVaCoAl’s CR_2 -based ordering the calculus pioneers—Leibniz (2), Euler (7), J. Bernoulli (7), Lagrange (17), Poisson (20)—all enter the top 20, whereas under a naive Python dict lexicographic ordering they are replaced by anatomists, surgeons, physicians, and humanists whose vote counts happen to survive the alphabetical cut, and Leibniz is demoted to rank 20 (Table 6). The broader methodological moral is general: on real data at a scale exceeding the writ of case-study investigation, path-dependence can arise not only from historical contingency but from the measurement architecture itself, and the constructive response is not to hope the architecture is innocent but to characterize its bias in closed form—here, a fourth-decimal-place per-step effect that the first-order historical findings overwhelm.

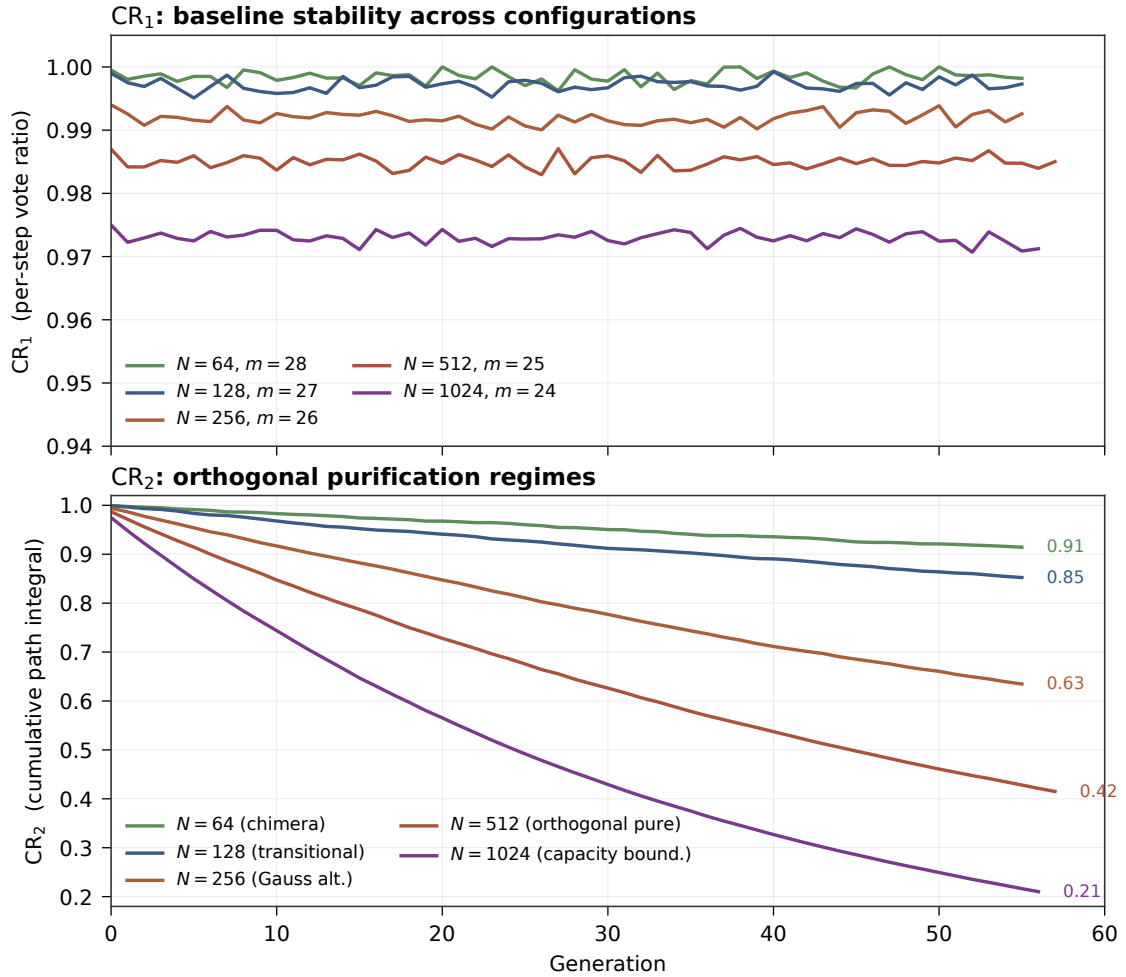


Figure 3: **CR₁ and CR₂ overlay across configurations.** CR₁ (upper band) stays near 1.0 regardless of dimensionality, confirming the macroscopic signal is never lost. CR₂ (lower trajectories) decays at rates depending on N : low- N configurations remain persistently high (the “chimera” regime); $N = 512$ shows steep yet smooth decay (orthogonal purification) and reaches the maximum depth of 57 generations; $N = 1024$ shows the steepest decay, the capacity boundary under $N \cdot 2^m = 2^{34}$.

Table 6: Top-20 vote comparison: PyVaCoAl ($N = 128, m = 27$, no rescue) versus Python dict. Votes in units of 10^4 .

| PyVaCoAl (no rescue) | | Python dict | | | |
|----------------------|---------------------|-------------|----|-------------------------|-------|
| Rk | Scholar (d.) | Votes | Rk | Scholar (d.) | Votes |
| 1 | J. Thomasius (1684) | 1,510 | 1 | J. Thomasius (1684) | 1,528 |
| 2 | Leibniz (1716) | 1,321 | 2 | B. Meisner (1626) | 1,378 |
| 3 | B. Meisner (1626) | 1,268 | 3 | C.A. Hausen (1743) | 1,339 |
| 4 | W. of Ockham (1349) | 1,214 | 3 | A.G. Kästner (1800) | 1,339 |
| 5 | Duns Scotus (1308) | 1,182 | 5 | A. Rhode (1633) | 1,167 |
| 6 | A. Hegius (1498) | 1,169 | 6 | A. Hegius (1498) | 1,140 |
| 7 | Euler (1783) | 1,054 | 7 | W. of Ockham (1349) | 1,092 |
| 7 | J. Bernoulli (1748) | 1,054 | 8 | Duns Scotus (1308) | 1,062 |
| 9 | T. à Kempis (1471) | 1,032 | 9 | J. Dubois (1555) | 1,060 |
| 10 | G. Groote (1384) | 1,015 | 10 | T. à Kempis (1471) | 1,012 |
| 11 | Gonsalvus (1313) | 1,003 | 11 | G. Groote (1384) | 992 |
| 12 | P. Olivi (1298) | 987 | 12 | Gonsalvus (1313) | 878 |
| 13 | C.A. Hausen (1743) | 970 | 13 | P. Olivi (1298) | 865 |
| 14 | A.G. Kästner (1800) | 968 | 14 | J. Peckham (1292) | 840 |
| 15 | A. Rhode (1633) | 961 | 15 | J.W.v. Andernach (1574) | 839 |
| 16 | J. Peckham (1292) | 957 | 16 | H. Fabricius (1619) | 835 |
| 17 | Lagrange (1813) | 945 | 17 | G. Falloppio (1562) | 832 |
| 18 | J. Martini (1649) | 944 | 18 | Bonaventure (1274) | 816 |
| 19 | Bonaventure (1274) | 928 | 19 | J.L. d'Étapes (1536) | 804 |
| 20 | Poisson (1840) | 903 | 20 | Leibniz (1716) | 787 |

3 Discussion

The network through which modern scientific knowledge was transmitted is not a web but a sequence of structural transitions. The 17th-century hourglass at Leibniz, with its 10:1 asymmetry, quantifies the multiplier that institutional integration applied to human-capital transmission; the 46-fold expansion in learned-society memberships across the same window, with six further independent indicators, supplies a structural anatomy of the institutional formation Mokyr (2016) identifies with the Republic of Letters. Reframed as transmission rather than priority, the Newton–Leibniz dispute admits a quantitative answer—Newton at rank 91, Leibniz at rank 2 on the Giant Score—that operationalizes the distinction between the *possession* and the *transmission* of upper-tail human capital. Upstream, 84% of lineages converge on five Islamic and Byzantine scholars who are less than 0.001% of the database, and the chain terminates at the 11th-century Monastery Wall, the more foundational of the two transitions.

For economists, the upshot is that “institutions” are not a residual category to be invoked after a discovery story is complete. The hourglass, the learned-society surge, and the multi-predicate continuity together depict a durable network good whose architecture changed at identifiable centuries. We do not estimate growth rates from the graph; the structural facts we report are a precondition for any growth narrative that would treat the cost of transmitting upper-tail human capital as endogenous, and they suggest concrete objects for identified follow-up work—for example, the formation of academies as a treatment whose downstream lineage effects are now, in principle, measurable.

Several limitations temper the findings. Wikidata’s recording biases—against non-Western, pre-university, and non-doctoral transmission—condition all results, though they work *against* our most striking upstream finding: a fuller archive could only dilute the apparent share of any specific chokepoint. We present no causal identification strategy; the findings are descriptive-

structural claims. The mentor–student predicate captures only one mode of transmission, and although we recover a second (books and translations) semantically, we have not mapped all modes. A different tracer set would change absolute counts and might shift the identities of the chokepoint individuals, but not the question of where the topology concentrates.

A word on responsible interpretation is in order, because macroscopic statistics can be misread as verdicts on whole cultures. Our graphs attach numbers to lineages *as Wikidata currently encodes them*, not to moral worth, civilizational ranking, or ancestry. A concentration of path traffic through a small set of pre-modern names is a fact about a database under a specific relation, and is best read as a symptom of who received documentary attention. The appropriate use of the finding is to generate disciplined hypotheses for historians, linguists, and area specialists. If a future release of Wikidata alters a handful of high-degree medieval edges and our contours move accordingly, that is a success of the programme, not a failure.

4 Conclusion

Working with all 64 historical Fields Medalists as a fixed, *ex ante* tracer set on the integrated Wikidata mentor–student graph, we have reconstructed for the first time at this scale the 25.5-million-path directed acyclic graph through which modern mathematical lineages connect to their pre-modern antecedents, and extracted three structural facts about the transmission of upper-tail human capital. They cohere into one picture. Across roughly nine centuries of documented mentorship, the social architecture of transmission did not evolve as a smooth gradient but moved through identifiable transitions: the 11th-century Monastery Wall, the prior condition at which personal academic lineage first becomes record-generating in Europe; and the 17th-century Leibnizian hourglass, through which an already-institutionalized regime acquired a 10:1 amplification, a 46-fold expansion in learned-society membership, and a coherent re-organization across seven predicate dimensions. Between Wall and hourglass, the highest-traffic individuals trace a profile that peaks in the 16th-century inception of the Scientific Revolution and yields to Leibniz alone thereafter. The Newton–Leibniz dispute, reframed under this geometry, resolves in favor of transmission over possession.

The instrument is a second contribution, but a subordinate one: a deterministic, algebraic graph-traversal method that makes exhaustive structural measurement on civilization-scale relational data feasible, and whose measurement bias is characterized in closed form rather than assumed away. We hope the larger methodological point outlasts the particular findings: that the economic history of knowledge now admits a structural, exhaustive mode of measurement, and that the facts it yields are the natural raw material for the identified, causal work the field does best.

CRediT authorship contribution statement

Hiroyuki Chuma: Conceptualization, Methodology, Software, Formal analysis, Investigation, Data curation, Writing – original draft, Writing – review & editing. **Kanji Otsuka:** Methodology (instrument architecture), Writing – review & editing. **Yoichi Sato:** Methodology (instrument architecture), Writing – review & editing.

Declaration of competing interest

The authors declare that they have no known competing financial interests or personal relationships that could have appeared to influence the work reported in this paper.

Funding

This research received no specific grant from any funding agency in the public, commercial, or not-for-profit sectors.

Acknowledgments

We thank the Wikidata, Mathematics Genealogy Project, and MacTutor History of Mathematics Archive communities for maintaining the data infrastructure upon which this study rests. We used Anthropic’s Claude AI assistant for Japanese-to-English translation and editorial assistance in the preparation of this manuscript. Additionally, Claude Code and the Cursor AI development environment were utilized to build our Python application, "PyVaCoAI." The authors retain full responsibility for all scientific claims, theorems, and proofs presented in this work.

Data availability

The underlying data are drawn from Wikidata, which is publicly available under a CC0 license. The Wikidata extraction queries (SPARQL), the genealogy-search configurations, the reference-vector specifications, the complete 64-Medalist tracer set, the PyVaCoAI reference implementation, and all tabular results reported here are deposited in a public repository (DOI to be assigned upon acceptance) and are available to editors and referees on request during peer review. All results are produced by a deterministic algorithm with no random seeds, so the reported figures are exactly reproducible from the deposited code and inputs.

Appendix. The appendices document the data construction (A–B), the deterministic graph-traversal instrument (C–G), the proofs (I), and the robustness checks and reproducibility detail (J–K) underlying the results in the body. Appendices C–G concern the measurement instrument; a reader interested only in the economic-history findings may treat them as supporting material.

Appendix A. Data

From Wikidata’s SPARQL endpoint (snapshot accessed 2026), we extracted all entities linked by the *doctoral advisor* (P184), *student* (P802), and *student of* (P1066) predicates within the network reachable from mathematics-oriented people. The raw dataset contained approximately 470,000 records. A pre-purification pass detected and removed 369 bidirectional links (cycles), yielding a clean directed acyclic graph (DAG) of 372,853 scholars. Wikidata’s systematic biases—over-representation of English-, German-, and French-language scholarship; denser modern than medieval records; better coverage of university-affiliated than court or non-Western practitioners—work against our Islamic convergence finding; the 84% rate is therefore a lower bound.

Appendix B. Genealogical search on a combinatorially explosive DAG

Starting from each of the 64 Fields Medalists, we traced mentor chains backward iteratively. Academic genealogy on the Wikidata mentor–student graph is not a tree: a scholar may have multiple recorded doctoral advisors; any given mentor typically has many students; and common ancestors propagate through overlapping descendant lineages. The resulting structure is a DAG in the strict mathematical sense, and the number of distinct paths from a source node to its ancestors grows multiplicatively with generational depth even when the number of distinct nodes is modestly bounded. Starting from 64 Fields Medalists on a DAG of 372,853 nodes, the path count reaches 25.5×10^6 at depth 57—a path-to-node ratio of approximately 68 : 1. A naive exhaustive search explodes well before this depth, so the search is executable only under a finite Frontier Size (FS) cap, which we set to 20,000. Every genealogical result in this paper is therefore FS-relative.

Failure of standard lookup primitives. We verified the failure of three standard alternatives under the data-scale conditions of our experiment. (i) Python hash tables: at FS = 25,000, the Python dict-based baseline exhausted 128 GB of main memory and became unexecutable. When dict runs at smaller FS, it ranks the within-FS candidates by lexicographic order of their identifiers, an ordering with no historical significance. (ii) GPU-based HDC libraries: the standard open-source framework `torchhd` (2023) requested over 100 GB of VRAM for the semantic-analysis stage and terminated with out-of-memory error on an NVIDIA RTX 3060 (12 GB VRAM); in GPU fallback mode, PCIe-bus bandwidth collapses the in-memory benefit entirely. (iii) Graph-theoretic centrality measures: PageRank and betweenness centrality complete in reasonable time on the full graph but are field-blind—they cannot distinguish a mathematician from an anatomist occupying the same topological position. None of these constraints reflects a poor tool choice; each is a direct consequence of the huge DAG structure of deep genealogical data interacting with the architectural assumptions of the standard toolkit (absolute exact match, decorrelated hashing, dense floating-point matrix operations). The methodological question for any instrument operating under the irreducible FS relativity imposed by the data is therefore: how are the within-FS candidates ranked, and does the ranking carry semantic content?

Appendix C. VaCoAI/PyVaCoAI architecture

We constructed an algebro-deterministic HDC architecture based on Galois-field algebra (2026) that replaces Kanerva’s probabilistic random projections (1988) with deterministic diffusion via Linear Feedback Shift Registers. For each of the approximately 1,043 hub individuals identified from the genealogy traffic, we attached up to 12 predicate dimensions via Wikidata SPARQL queries (academic field, language used, employer institution, society membership, era, birthplace, and others). Attributes were encoded as million-dimensional binary hypervectors and subjected to Binding, Unbinding, and Bundling operations, enabling continuous measurement of each node’s affinity to specific intellectual traditions via Hamming-distance similarity. The entire computation completed in 20–30 minutes on a decade-old Intel Xeon E5-1650 v3 (2014) with no GPU.

Galois-field diffusion. Input data $P(x)$, represented as a binary polynomial over GF(2) with coefficients $a_i \in \{0, 1\}$, is mapped to a high-dimensional vector via

$$F(x) = x^m P(x) + (x^m P(x) \bmod G(x)), \quad (3)$$

where $G(x)$ is a degree- m generator polynomial drawn from the class of long-period polynomials over $\text{GF}(2)$. The choice of a finite field rather than an unbounded ring is structural: the mod $G(x)$ operation ensures that the transformation cycles within a bounded address space, and it is precisely this cycling within a closed world that scatters similar inputs into mutually unrelated directions, creating orthogonality *algebra-deterministically*. The operation is implementable as a single LFSR pass whose hardware cost is negligible. Under the primitive-polynomial conditions detailed in (2026), a single-bit input change triggers the *avalanche effect*: approximately 50% of output bits flip.

Per-block diffusion. The input hyper-vector is partitioned into N segments of length $q = L/N$ (main analysis uses $N = 128$, $q \approx 8000$, $L \approx 10^6$). Each block b applies its own independent LFSR diffusion with its own feedback polynomial $G_b(x)$ and its own seed, producing an m -bit address. This per-block architecture is structurally necessary: under a hypothetical global diffusion, a single-bit perturbation of the input would, by the avalanche effect, propagate to all N block addresses, corrupting every vote. Under the per-block diffusion actually implemented, such a perturbation affects only the one or two blocks whose segments contain the flipped bit; the remaining $N - O(1)$ blocks continue to output the correct entry address, and the avalanche effect within the affected blocks diffuses their erroneous votes uniformly across the address space.

Block division and majority voting. Each of the N blocks (64–1,024 in our experiments) functions as an independent SRAM/DRAM lookup table with 2^m entries. In the write phase, a unique Entry Address (EA) is written to the addressed location in every block. In the read phase, each block i votes for an EA v_i :

$$W_{\text{VaCoAl}} = \arg \max_v \sum_{i=1}^N \delta(v_i, v), \quad (4)$$

where δ is the Kronecker delta. Erroneous votes scatter uniformly across the address space (a flat field), while correct votes concentrate on a single peak.

Collision tolerance and the rescue circuit. When different items map to the same block address, VaCoAl marks the block as *Don't Care* and excludes its vote from the aggregation in that retrieval step. Under multi-hop reasoning, this acquires a second-order property whose closed-form magnitude appears in Appendix F. In the complementary *Rescue* mode (rescue rate $\text{RR} > 0$), a four-stage pipeline explicitly intercepts and resolves collisions: sample accumulation at write time; per-block address-sorted finalisation; binary search at query time against per-block auxiliary arrays; and segment exact match within each candidate interval. With $\text{RR} = 1$ this pipeline pins $\text{CR}_1 \equiv 1.0$ and produces output bitwise identical to the Python `dict` baseline (verified across all 25.5×10^6 records). Main-text analysis uses $\text{RR} = 0$.

HDC algebraic operations. Three operations are central to the semantic analysis: *Binding* ($A \otimes B$) via XOR and cyclic shift over $\text{GF}(2)$, at cost $O(N)$; *Bundling* ($A + B$) via component-wise majority vote; and *Unbinding* as the inverse of Binding, exploiting the algebraic reversibility of XOR over $\text{GF}(2)$ for lossless concept decomposition. Similarity is measured by Hamming distance; for quasi-orthogonal vectors in an L -dimensional binary space, the expected similarity between uncorrelated vectors is 0.5.

Equation (3) is formally identical to the systematic-code form of a BCH code, yet the purpose is diametrically opposite. BCH codes expend elaborate computation (syndrome decoding) to force convergence to a unique correct codeword. VaCoAl abandons this convergence logic and uses Galois-field operations as a *scoreboard* for relative similarity and path quality. On massive

DAGs subject to combinatorial explosion, an absolute exact match cannot in principle exist; VaCoAl embeds a cognitive bound—the Frontier Size—into the architecture and ranks within-FS candidates by the path-integral score CR_2 .

Appendix D. Confidence scores

The architecture produces two confidence scores: CR_1 is the block-majority-voting rate at a single retrieval step; $\text{CR}_2(n) = \text{CR}_2(n-1) \cdot \text{CR}_1(n-1)$ is the generational product, a path integral that accumulates confidence multiplicatively along a chain. In Rescue mode, $\text{CR}_1 \equiv 1.0$ identically. In Don’t Care mode with the $(N = 128, m = 27)$ configuration, $\text{CR}_1 \approx 0.995\text{--}0.999$; the residual per-block collisions contribute the minute analog variance. Within-FS candidate ranking is by CR_2 ; hash-based baselines lack any such score and fall back to lexicographically vacuous ordering. At sufficient memory depth $\text{CR}_1 \approx 0.997$, yielding the closed-form prediction $\text{CR}_2(n) \approx 0.997^n$ that matches measured values across all 25.5×10^6 paths.

Appendix E. Mathematical isomorphism with biological neurons

The output y_{bio} of a biological neuron is the application of a nonlinear activation φ to the inner product of input $\mathbf{x} \in \mathbb{R}^D$ with synaptic weights $\mathbf{w} \in \mathbb{R}^D$: $y_{\text{bio}} = \varphi(\mathbf{w} \cdot \mathbf{x} - \theta)$. For HDC bipolar vectors $\{-1, +1\}^D$, the inner product relates linearly to Hamming distance: $\mathbf{w} \cdot \mathbf{x} = D - 2 d_H(\mathbf{w}, \mathbf{x})$. In VaCoAl, with $\delta_i \in \{0, 1\}$ the match decision for block i , $y_{\text{vac}} = \mathbb{I}\left(\sum_{i=1}^N \delta_i > \theta_{\text{digital}}\right)$. By the Law of Large Numbers and the uniform error distribution guaranteed by Galois-field diffusion, the vote count is a strictly monotone increasing estimator of $\mathbf{w} \cdot \mathbf{x}$, yielding $y_{\text{vac}} \equiv \mathbb{I}(\mathbf{w} \cdot \mathbf{x} > \theta_{\text{analog}})$ —formally identical to the biological rule. Mapping PyVaCoAl’s processing onto the three-layer structure of a pyramidal neuron yields a structural flow equivalence (dendrites \rightarrow soma \rightarrow axon corresponds to per-block exact match \rightarrow majority voting on $\text{CR}_1 \rightarrow \text{CR}_2$ propagation), not a strict dynamical isomorphism: dendrites exhibit graded NMDA nonlinearities and somatic integration is distance-weighted, while VaCoAl’s checking is discrete and its voting equal-weight. We further note a biological homology in the substitution of a fixed algebraic logic circuit for stochastic random projection: Fiete et al. (2008) and Chandra et al. (2025) show that the Residue Number System code formed by grid cells in the entorhinal cortex is projected onto hippocampal CA3 as a fixed random projection, completed during early childhood; subsequent memory processes execute as orthogonalising mappings onto the invariant vessel. VaCoAl’s LFSR-on-SRAM/DRAM realisation of orthogonalisation is, in this sense, a digital-logic reproduction of this biological finding—an instance of what we call *convergent computational equivalence*. Compared with Eliasmith’s Semantic Pointer Architecture (2013), which solves the Binding Problem (2019) via circular convolution at $O(N \log N)$ FFT cost with floating-point arithmetic, VaCoAl provides an algebraically reversible solution via Galois-field XOR and shift at $O(N)$ bitwise cost at single-bit precision.

Appendix F. Emergent semantic selection: multi-configuration phase transitions

Under a fixed total-capacity constraint $N \cdot 2^m = 2^{34}$ (corresponding to 64 GB DRAM per the $(128, 27)$ realisation), the system does not simply degrade monotonically as the per-block collision rate rises; it undergoes four macroscopic topological phase transitions, each preserving a distinct, historically valid lineage structure (Table 7).

Chimera state ($N = 64$). In the lowest-dimensionality regime ($N\text{-dim} = 6,400$), the system lacks the orthogonal resolution to separate massive overlapping subgraphs. Traversal produces a fragmented superposition that fuses German lineage elements (Hausen, Kästner) with analytical elements (Thomasius) while losing the central hub Leibniz entirely.

Transitional emergence ($N = 128$, *main analysis*). Orthogonal resolution at $N\text{-dim} = 12,800$ suffices to identify the primary macroscopic structure. The Leibniz lineage emerges strongly (Leibniz, Euler, J. Bernoulli), but residual Gauss-lineage crossover nodes (Hausen, Kästner) still persist within FS due to incomplete culling.

Bifurcation and alternate attractor ($N = 256$). The specific analog-noise profile at 0.282% collision rate alters the CR_2 fitness landscape. At critical historical bifurcations, this configuration marginally favours the alternative subgraph: the Leibniz lineage is culled, and the lineage of Carl Friedrich Gauss (Pfaff, Hausen, Kästner) emerges instead—an alternate, historically accurate macroscopic structure.

Orthogonal purification ($N = 512$). At $N\text{-dim} = 51,200$ and collision rate 0.559%, robust orthogonality subdues the interference entirely. The system converges definitively on the Leibniz–Euler lineage and purifies the extraction down to Lagrange and Poisson. This is the only VaCoAl configuration matching the maximum genealogical depth of 57 generations attained by the `dict` baseline at $\text{FS} = 20,000$.

Capacity boundary ($N = 1024$). Extending N to 1024 halves m from 25 to 24 and doubles the count-based collision rate to 1.108%. The Leibniz-dominant regime is retained, but the reachable depth drops to 56.

Table 7: Collision-rate analysis under fixed total capacity $N \cdot 2^m = 2^{34}$, and the empirical regime it produces.

| Configuration | Loc. rate | Count rate | Depth | Regime |
|--------------------|-----------|------------|-------|-------------------------|
| $N = 64, m = 28$ | 0.000103% | 0.074% | 55 | Chimera |
| $N = 128, m = 27$ | 0.000399% | 0.144% | 55 | Leibniz dominant (main) |
| $N = 256, m = 26$ | 0.001565% | 0.282% | 55 | Gauss dominant |
| $N = 512, m = 25$ | 0.006189% | 0.559% | 57 | Orthogonal purification |
| $N = 1024, m = 24$ | 0.024437% | 1.108% | 56 | Capacity boundary |

Three conclusions follow. (i) High collision rates are not the enemy; the quadrupling of the count-based collision rate from $N = 128$ to $N = 512$ *improves* rather than degrades semantic purity. (ii) The Don’t-Care-driven STDP-like decay is not a blunt instrument; a deep path with coherent CR_2 mass along a truly continuous academic lineage survives, while a similarly deep path traversing ancient junctions without semantic continuity is eliminated. (iii) The optimal balance under a fixed-capacity budget is a trade-off between orthogonal resolution (scaling with N) and per-block collision tolerance (scaling with 2^m)—not maximising either factor in isolation.

Speed and the FS phase transition. A phase transition occurs at $\text{FS} \approx 20,000$: `dict` is faster below this threshold, PyVaCoAl overtakes above it; at $\text{FS} = 25,000$, `dict` exhausts 128 GB and fails while PyVaCoAl completes stably. On the HDC semantic-analysis stage, the CPU-only `torchhd` baseline required ~ 60 min ($2 \times$ PyVaCoAl’s ~ 30 min); the GPU variant terminated with OOM after requesting > 100 GB of VRAM.

Appendix G. Functional equivalence to STDP and CA3 recurrent collaterals

Spike-Timing-Dependent Plasticity (1998) in biological neural circuits is often described as a physical mechanism of analog synaptic dynamics. Abstracting away the implementation substrate, the computational problem it solves is: *in multi-stage information transmission, exponentially decay the weight of a path according to its distance from the starting point, selectively preserving close, direct paths*. Under this abstract specification, the STDP function does not inherently depend on millisecond-precision analog spikes but on the computational structure of distributed representation and threshold judgement; implementations are therefore not limited to analog circuits. The most important characteristic of CA3 recurrent-collateral integration emphasised by Rolls (2023) is the recursion by which past computational results are fed back into current pattern completion. The update rule in PyVaCoAl is formally isomorphic: the cumulative confidence of the previous generation, $CR_2(n-1)$, is recursively fed into the computation for the next generation, and only candidates surviving CR_1 , CR_2 , and the FS cap become search starting points for the next generation. Three functional parallels with CA3 obtain: full-pattern completion from partial patterns; natural suppression of sub-threshold patterns (halting at $CR_2 < 0.10$); and winner selection among competing patterns (Don't Care defers premature commitment). This is convergent computational equivalence, not mimicry: different implementation substrates arrived at the same functional structure by independently solving the same computational problem. The digital algebraic implementation acquires three properties unachievable in principle by analog neuromorphic implementations: *perfect reversibility* (Binding/Unbinding via GF(2) XOR and shift is algebraically reversible); *mathematical auditability* (the CR_2 path integral permits algebraic backtracking of why a given answer was produced); and *deterministic zero-collision guarantee* in Rescue mode (verified empirically across all 25.5×10^6 records).

Appendix H. HDC signal trace of the Great Translation Movement

The mentor–student predicate captures only one channel of knowledge transmission. The Great Translation Movement of the 12th century transmitted knowledge through books and translators, not personal mentorship, and is therefore by construction invisible to a mentor–student genealogy. We recover this transmission channel indirectly through HDC semantic analysis: for each 50-year window W_k , we Bundle the composite $H(W_k)$ over all scholars active during the window (birth-year overlap) and Unbind the FIELD component. The signal at window k for field $F \in \{\text{algebra, astronomy}\}$ is

$$\sigma_F(k) = \frac{1}{L} \sum_{i=1}^L \mathbb{I}(\text{Unbind}(H(W_k), \text{FIELD})_i = \text{Ref}_{F,i}), \quad (5)$$

where Ref_F is the field-specific reference vector. The astronomy signal surges during 1250–1300 (+0.0025, coinciding with the second Toledo translation period and the peak of the Maragha observatory school) and again during 1450–1500 (+0.0065, the Renaissance peak overlapping with Copernicus's lifetime). Algebra shows no comparable surge. Copernicus's documented borrowing of the mathematical models of al-Urdī (1200–1266), al-Ṭūsī (1201–1274), and Ibn al-Shāṭir (1304–1375) (2007)—composed 200–300 years before his time and translated from Arabic into Latin via intermediaries—is consistent with the semantic trace detected at 1250–1300 and its Renaissance amplification. The asymmetry between algebra and astronomy is therefore

a substantive observation rather than a by-product of window width: a flat discipline would wobble near the random 0.5 line, whereas astronomy repeatedly departs in the same direction whenever translation episodes and Copernican-era activity plausibly raised the public salience of instruments, tables, and geometrical models. The exercise does not prove that any individual Medalist’s intellectual DNA passed through a Toledo manuscript; it shows that, at population level, the semantic field vector tilts in a way that a purely topological graph test could never register.

Appendix I. Proof: false-positive probability vanishes asymptotically

Galois-field diffusion distributes random noise uniformly across the address space of size $M = 2^m - 1$. The per-block false-positive rate is $p = 1/M$. Per-block diffusion ensures that a single-bit perturbation affects only $O(1)$ blocks whose segments contain the flipped bit; the remaining $N - O(1)$ blocks output the correct Entry Address. Within the affected blocks, the avalanche effect diffuses erroneous votes uniformly, producing the flat-field noise distribution on which the Chernoff bound relies. The number of accidental coincident votes X follows Binomial(N, p). In the worst case $N = M = 1,000$: mean $\mu = Np = 1$, majority threshold $\theta = 500$, deviation $\delta = 499$. By the multiplicative Chernoff bound,

$$P_{\text{error}} = P(X \geq \theta) \leq \left(\frac{e^\delta}{(1 + \delta)^{1+\delta}} \right)^\mu, \quad (6)$$

yielding $\ln P_{\text{error}} \approx 499 - 500 \ln(500) \approx -2606$ and $P_{\text{error}} \leq e^{-2606} \approx 0$. This bound is more than 2,500 orders of magnitude smaller than the probability of randomly selecting a specific atom from the observable universe ($\approx e^{184}$). Noise-induced majority false positives in VaCoAl are, for all practical purposes, impossible: the gap between noise floor ($\mu = 1$) and majority threshold ($\theta = 500$) is insurmountable by probabilistic fluctuations alone.

Appendix J. Robustness checks

Frontier Size sensitivity. Results are qualitatively stable across $\text{FS} \in \{10,000, 15,000, 20,000\}$. At $\text{FS} = 25,000$ the Python `dict` baseline fails (OOM), but PyVaCoAl still produces stable figures. The 84% Islamic convergence reported in the main text ranges from $\sim 72\%$ at $\text{FS} = 5,000$ to 84% at $\text{FS} \geq 10,000$, plateauing thereafter.

Rescue Rate sensitivity. Between $\text{RR} = 0$ (pure Don’t Care; main analysis) and $\text{RR} = 1$ (full Rescue, eliminating the CR_2 penalty), all main-text historical findings are preserved nearly bit-identically: the 84% Islamic convergence, the Leibniz 10:1 hourglass, the Monastery Wall, the 46-fold society-membership explosion, the Newton rank of 91 on the Giant Score. The difference between the two modes appears especially in the within-FS ranking of sub-threshold candidates, precisely where CR_2 adds semantic content (Table 6).

Memory-depth sensitivity and reachable depth. PyVaCoAl is not a static hash-matching algorithm but a dynamic topological scanner. Across all configurations from $N = 64$ ($N\text{-dim} = 6,400$) to $N = 1024$ ($N\text{-dim} = 102,400$), CR_1 remains overwhelmingly stable above 0.975, confirming that the system never loses the core macroscopic signal despite the intentional compression of memory depth. The CR_2 trajectories reveal the definitive signature of dimensional filtering: $N = 64$ retains persistently high CR_2 (chimera state, lacking orthogonal resolution); $N = 512$ undergoes a steep yet smooth decay (the mathematical manifestation of orthogonal

purification, in which the high-dimensional space actively filters out residual interference and isolates the true analytical trajectory); $N = 1024$ shows the steepest decay, reaching the capacity boundary. Viewed across all configurations, the reachable depth is non-monotonic in N : 55 generations for $N = 64, 128, 256$; 57 for $N = 512$; and 56 for $N = 1024$. $N = 512$ is the only configuration matching the maximum depth of 57 generations attained by Python dict at FS = 20,000. This non-monotonicity is shown explicitly in the main-text Fig. 3 overlay and the per-generation trajectories of Fig. 2.

Alternative tracer sets. Although a full head-to-head replication with a different tracer set (e.g., Nobelists in physics) is beyond the scope of the present paper, the structural logic of the exercise—that a fixed, ex ante tracer set induces a well-defined subgraph on a DAG too large for unaided intuition—does not depend on the particular choice of Fields Medal. The Wikidata predicates (P184, P802, P1066), the DAG structure, the combinatorial explosion, and the FS relativity apply identically to any modern elite science tracer set. A different tracer set would yield different absolute chokepoint identities; the methodological architecture reported here would be unchanged.

Appendix K. Reproducibility

The complete algorithmic specification of VaCoAl/PyVaCoAl—including the primitive-polynomial construction of the Galois-field diffusion, the per-block LFSR addressing, the four-stage Rescue pipeline, the HDC Binding/Unbinding/Bundling operations at single-bit precision, and the CR₁/CR₂ computation—appears in the companion preprint (2026) at a level of detail sufficient for independent reimplementations. Wikidata extraction queries (SPARQL), genealogy-search configurations, HDC reference-vector specifications, the complete 64-Medalist tracer set, and all tabular results of the present paper are released as Supplementary data on a public repository (DOI to be assigned at acceptance) and made available to editors and reviewers upon request during peer review. The combination of algorithmic disclosure, public input data, deterministic algorithm (no random seeds), and explicit closed-form bias characterisation satisfies the reproducibility standard appropriate to a paper whose findings are structural rather than statistical-inferential.

References

- Mokyr J (2002) *The Gifts of Athena: Historical Origins of the Knowledge Economy*. Princeton Univ. Press.
- Mokyr J (2016) *A Culture of Growth: The Origins of the Modern Economy*. Princeton Univ. Press.
- Saliba G (2007) *Islamic Science and the Making of the European Renaissance*. MIT Press.
- Itoh S (1993) *The Twelfth-Century Renaissance: The World of Arabic Civilisation and Western Europe*. Iwanami Shoten. [In Japanese.]
- Squicciarini MP, Voigtländer N (2015) Human capital and industrialization: Evidence from the age of Enlightenment. *Q. J. Econ.* 130:1825–1883.
- Dittmar JE (2011) Information technology and economic change: The impact of the printing press. *Q. J. Econ.* 126:1133–1172.

- Cantoni D, Yuchtman N (2014) Medieval universities, legal institutions, and the commercial revolution. *Q. J. Econ.* 129:823–887.
- Heddes M, et al. (2023) Torchhd: An open-source Python library to support research on hyper-dimensional computing and vector symbolic architectures. *J. Mach. Learn. Res.* 24:1–10.
- Chuma H, Otsuka K, Sato Y (2026) Beyond LLMs, sparse distributed memory, and neuromorphics: A hyper-dimensional SRAM-CAM “VaCoAI”. arXiv preprint arXiv: <https://arxiv.org/abs/2604.11665> [cs.NE].
- Kanerva P (1988) *Sparse Distributed Memory*. MIT Press.
- Bi G-q, Poo M-m (1998) Synaptic modifications in cultured hippocampal neurons: Dependence on spike timing, synaptic strength, and postsynaptic cell type. *J. Neurosci.* 18:10464–10472.
- Hall AR (1980) *Philosophers at War: The Quarrel Between Newton and Leibniz*. Cambridge Univ. Press.
- Rashdall H (2010) *The Universities of Europe in the Middle Ages*, 3 vols. Cambridge Univ. Press [originally 1895].
- De Ridder-Symoens H, ed. (1992) *A History of the University in Europe, Vol. 1: Universities in the Middle Ages*. Cambridge Univ. Press.
- Rolls ET (2023) *Brain Computations and Connectivity*, 2nd ed. Oxford Univ. Press.
- Fiete IR, Burak Y, Brookings T (2008) What grid cells convey about rat location. *J. Neurosci.* 28:6858–6871.
- Chandra S, Sharma S, Chaudhuri R, Fiete I (2025) Episodic and associative memory from spatial scaffolds in the hippocampus. *Nature* 638:739–751.
- Eliasmith C (2013) *How to Build a Brain: A Neural Architecture for Biological Cognition*. Oxford Univ. Press.
- Thagard P (2019) *Brain–Mind: From Neurons to Consciousness and Creativity*. Oxford Univ. Press.